Electrical Conductivity of Olivine[1]

AL DUBA[2]

Hoffman Laboratory, Harvard University, Cambridge, Massachusetts 02138

The electrical conductivity σ of single crystals of olivine of 0, 7.7, 8.2, 9.4, and 26.4 mole % fayalite has been measured up to 1200°C and 7.5 kb. Samples from different localities with approximately the same fayalite content and impurity levels have electrical conductivities that differ by 2–3 orders of magnitude. It is proposed that the oxidation state of the iron in the natural olivines determines σ below 1100°C. No reversible change in activation energy was noted for any sample below 1100°C. In this temperature range activation energies for different samples vary from 0.7 to 2.0 ev. At 1150°C there is a reversible increase in σ with a poorly determined activation energy of 7–8 ev. Mantle temperatures calculated from the present data on olivines with almost the same fayalite content differ by more than 700°C at any depth. The temperature difference becomes even larger with depth if the pressure effects noted in this study are used.

The distribution of electrical conductivity σ in the mantle has been calculated from geomagnetic and magnetotelluric data by using inversion techniques [*Banks*, 1969; *Price*, 1967; *Eckhardt et al.*, 1963; *McDonald*, 1957]. With these models of mantle σ, limits can be set on the temperature distribution in the mantle, provided that the σ of mantle constituents is determined as a funcion of temperature and pressure.

The geophysical and geochemical evidence that olivine is the major phase of the earth's upper mantle is overwhelming [*Wyllie*, 1970; *Birch*, 1969; *Ringwood*, 1969; *Harris et al.*, 1967]. Although the entire range of the forsterite-fayalite solid solution (Mg_2SiO_4-Fe_2SiO_4) occurs in metamorphic and igneous rocks, the most common composition of olivine in ultramafic intrusions, nodules in basalts, and kimberlites is $\simeq 10$ mole % fayalite (Fa 10) and thus is probably the composition of the olivine in the mantle [*Fujisawa*, 1968].

Because the major continuous phase in any mixture of minerals determines the σ of the mixture [*Volarovich et al.*, 1966; *Tozer*, 1959; *Hughes*, 1953], the investigation of the σ of

mantle constituents can be limited to olivine. This limitation simplifies the experimental procedure, because small thin single-crystal specimens can be used. Thus the problems of large temperature gradients across representative rock samples and the shunting effect of the larger sample holder required for large specimens are eliminated.

In line with the above considerations three olivines with compositions of about Fa 10, an olivine with a composition of Fa 26, and a Linde synthetic forsterite were studied. The concentration on the Fa 10 composition was deliberate, because this composition of olivine in the mantle is most likely. Also the largest unzoned inclusion-free samples could be prepared from olivines of this composition. The high-fayalite sample and synthetic forsterite were chosen to permit evaluation of the effect of fayalite content on the σ. (These samples are described in Tables 1 and 4.)

Previous studies of the σ of olivine have concentrated mainly on synthetic and natural powders [*Akimoto and Fujisawa*, 1965; *Bradley et al.*, 1962, 1964; *Hamilton*, 1965; *Jander and Stamm*, 1932; *Pluschkell and Engell*, 1968; *Schult and Schober*, 1969]. The use of powdered samples permits study of the entire olivine solid solution and the utilization of solid-pressure media to achieve pressures up to 65 kb. Unfortunately grain-boundary effects and compaction problems may cause powder data to be nonrepresentative of the electrical properties of

the single crystals [*Rodgers et al.*, 1966; *Hutson*, 1959].

Work on single crystals has been limited to a study by *Hughes* [1955] of gem-quality peridot up to 8 kb from 1060° to 1240°C, atmospheric-pressure studies of natural olivine by *Hughes* [1953], *Noritomi* [1961], and *Mizutani and Kanamori* [1967], and studies of forsterite grown by the flame-fusion method and doped with small amounts of iron [*Shankland*, 1969]. (The literature data on the conductivity of single crystals are included in Figure 3.)

If the logarithm of the σ of olivine is plotted against reciprocal temperature, the data lie on nearly straight lines or straight-line segments. Thus σ can be expressed as

$$\sigma = \sigma_x \exp\left(-A_x/kT\right) \qquad (1)$$

where the coefficient σ_x is independent of temperature, A_x is the activation energy, k is Boltzmann's constant, and T is the temperature in degrees Kelvin. The subscript x indicates that more than one conductivity mechanism may be operating. These mechanisms include ionic conduction and extrinsic and intrinsic electronic semiconduction. For a more complete description of the various σ mechanisms possible in olivine see *Hamilton* [1965]. *Kittel* [1966] and *Dekker* [1958] describe in considerable detail the σ of semiconductors. Olivine may be classified in this category.

SAMPLE PREPARATION

Single crystals of olivine were cut in thin slices (<0.02 cm) by a 0.006-inch diamond wheel turning at very slow speeds with low feeding pressures to minimize crystal damage. These slices were then carefully hand-lapped with a final alumina grit of 0.05 μ. The olivine sections were cleaned thoroughly with acetone and washed ultrasonically in a soap solution and in ethyl alcohol to ensure a clean surface on which to apply the conductive coating of platinum. Before being plated with platinum, the crystals were examined optically for flaws such as cracks, inclusions, and alteration products.

Two methods of platinum plating were used. Crystals from the San Carlos Indian reservation were painted with Liquid Bright, a platinum paint produced by DuPont de Nemours Company. Repeated applications of the paint and firing to 600°C in air resulted in a thick platinum coat on the crystal surfaces. An uncoated thin section of olivine showed no color change during this procedure; thus it is assumed that there was no oxidation of olivine during this coating process. The remaining samples were placed in a bell jar, evacuated to about 10^{-6} atm, and ion-bombarded to ensure a clean surface on which to deposit platinum. The crystals were then heated to 800°C by a tantalum-strip heater, and platinum-charged tungsten wires 4 cm above the crystals were heated sufficiently to evaporate platinum onto the crystals.

The platinum-coated plates of olivine were then cut into parallelograms whose lateral dimensions were in most cases at least 10 times their thicknesses to avoid boundary effects. Thickness and area were measured with a traveling microscope marked in 0.0001-inch intervals.

The orientation of the olivine samples was determined by the Laue back-reflection technique to within 0.5° and was checked by precession techniques. Table 1 lists sources, localities, and chemical compositions for samples used in this study.

EXPERIMENTAL APPARATUS

Figure 1 shows the sample-holder assembly with the primary and secondary heaters. The assembly was designed so that its conductance, which increases with temperature, would not interfere with the conductance measured for the olivine. Thus care was taken to ensure that no contact was made between the ceramic parts that carried the electrodes contacting the sample or between either ceramic piece and the furnace in the hot regions. This lack of contact was accomplished by making the inner parts of the assembly as concentric as possible with the furnace and by allowing relatively large clearances in the central parts and little clearance at the ends.

The leakage conductance between the electrodes with no sample inserted was measured in two separate runs and is given in Table 2, with data from the measurements of olivine conductance for comparison. Only conductances greater than the leakage conductance by at least 2 orders of magnitude were considered in the σ calculations. For the Fa 0 and the Fa 9.4 this leakage conductance was not negligible

TABLE 1. Sample Description

Sample	Locality	Source	Composition
12	Mt. Leura, Camperdown, Victoria, Australia	Mineral collection, Dep. of Geophys. Sci., Univ. of Chicago	Fa 7.7
18	San Carlos Indian Reserv., Ariz.	E. J. Olsen, Field Mus. of Natural Hist., Chicago	Fa 8.2
35	St. John's Island, Red Sea, Egypt	Mineral collection, Dep. of Geophys. Sci., Univ. of Chicago	Fa 9.4
36	Crater Elegante, Sierra Del Pinacote volcanic field, Sonora, Mex.	D. Johnson, Geol. Dep., Stanford Univ., Palo Alto, Calif.	Fa 26.4
38	Synthetic forsterite (grown by Linde flame-fusion process)	O. L. Anderson, Lamont-Doherty Geol. Observ., Columbia Univ., Palisades, N. Y.	Fa 0 (wt %: SiO_2, 43.02; MgO, 56.82; MnO, 0.16; others, <0.01*)

*From *Kumazawa and Anderson* [1969].

below 700° and 500°C, respectively, but in all other instances effects of leakage conductance vanished above about 200°C.

Since the temperature gradient may be quite large in this simple furnace, accurate temperature measurement at the sample was necessary. This accuracy was accomplished by having the chromel-alumel thermocouple contact the sample and serve as one electrode. A new thermocouple was used for each sample; these thermocouples were calibrated at the NaCl melting point, and the reported temperatures are believed to be correct to within 2°–3°. Temperature readings were corrected for the effect of pressure on chromel-alumel thermocouples [*Getting and Kennedy*, 1971].

Carbon from trace amounts of hydrocarbons in the argon and 'O'-ring 'dust' from intensifier packings were major problems in these experiments. Many experiments were terminated at about 500°C when a thin carbon film was deposited in the sample region and the measurement was shorted out. Secondary heaters, both with and without titanium-zirconium alloy getters, were ineffective, as was running the primary heater at elevated temperatures and allowing the carbon to deposit in the cooler regions of the furnace away from the crystal, as was suggested by *Hughes* [1955]. The method that effectively removed the carbon was the introduction of a small amount of oxygen (less than 0.03%) into the argon to oxidize the hydrocarbon in a secondary furnace located in the pressure vessel away from the sample.

The introduction of oxygen into an atmosphere in which one is measuring the σ of a semiconductor such as olivine will affect the conductivity [*Shankland*, 1969; *Pluschkell and Engell*, 1968; *Hamilton*, 1965]. Irreversible σ changes in the samples were checked experimentally by continuously cycling back to lower temperatures after every 100°–200°C increase in temperature and repeating measurements. In this way one could easily detect chemical change due to oxidation of the olivine (or to the appearance of carbon), because irreversible increase in conductance ensued in either case. Carbon began to appear above 500°C, and oxidation was noted to begin at about 800°C, both temperatures being somewhat dependent on oxygen content.

Confining pressures were generated in standard separators and intensifiers, in which argon was the pressure medium. Pressure was measured by the resistance change of a manganin coil that had been calibrated against a 7-kb Heise pressure gage with an accuracy of 0.1%. The accuracy of the pressure measurement is better than 0.5%, and precision is 0.1%.

Conductance was measured at 1000 Hz and 30 volts with a General Radio 1615-A capacitance bridge with a stated accuracy of 1%. The σ measured was assumed to be independent of
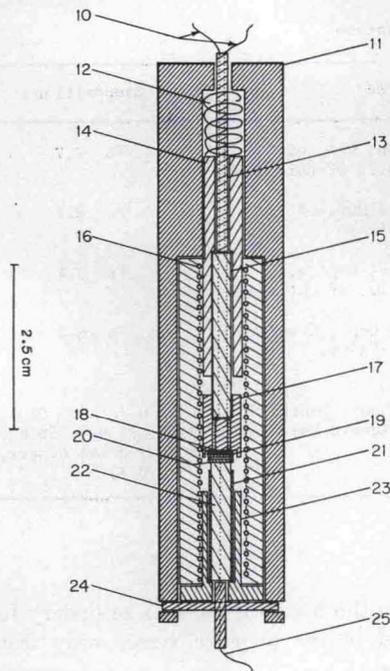
Fig. 1. Sample holder. Numbers on the diagram are as follows: 10, thermocouple leads; 11, lavite cylinder; 12, steel spring; 13, alumina tubing; 14, bottom lavite cap; 15, alumina tubing; 16, primary furnace; 17, alumina crystal holder; 18, chromel-alumel thermocouple; 19, olivine crystal; 20, platinum electrode; 21, 0.001-inch tungsten foil; 22, alumina tubing; 23, top lavite cap; 24, nickel rod; and 25, platinum wire to electrode.

frequency, as was indicated by the results of *Hamilton* [1965] and *Bradley et al.* [1964] for powders. Conductances of 10^{-3} mho and greater were measured with a circuit similar to that used by *Schock* [1966]. The σ is calculated from the measured conductance

$$\sigma = G(t/A) \qquad (2)$$

where t is the thickness and A is area of the sample.

EXPERIMENTAL PROCEDURE

In a typical run the oxygen was introduced into the first-stage argon compressor to yield a mix of argon to oxygen of 3.6×10^2. The system was then pressurized to 7.5 kb, and the secondary furnace was heated to about 1000°C for 1 hour before σ measurements were begun. Measurements were made as a function of temperature at constant pressure; temperature

cycles were reversed every 100°–200°C to verify reproducibility and to check for anomalous behavior due to the presence of excess carbon or oxygen. After achieving a temperature of 750°C at 7.5 kb, the temperature was lowered to around 100°C, the pressure was lowered to 5.00 kb, and the procedure was repeated. For all compositions except the Fa 7.7 olivine runs were made at 7.50, 5.00, and 2.50 kb. Runs at 7.50 kb were made with at least two different samples for each crystal direction to determine the variation of σ with direction for the Fa 8.2. Reproducible data at temperatures greater than 1000°C were achieved only for the Fa 0 and the Fa 9.4. The chief limiting factor for the runs made at higher temperature was oxidation of the crystal or the thermocouple or both.

DATA AND ANALYSIS

Figure 2 illustrates the σ of olivine as a function of temperature, pressure, and composition for all samples studied. Lines are plotted from a linear-regression analysis of the σ data. Equations of the lines shown in Figure 2, along with standard deviations, can be found in Table 3. Because the pressure variation of the Fa 8.2 is so small, it is not plotted in Figure 2.

With the exception of the Fa 9.4, the σ has a tendency to increase with fayalite content. The Fa 26.4 and the Fa 9.4 single crystals do not fit the behavior of powders in which activation energy decreases with iron content [*Bradley et al.*, 1964], although the other three compositions do follow this behavior.

The difference in activation energies for σ in olivines with almost the same iron content is puzzling and might seem to be due to impuri-

TABLE 2. Leakage Conductance

Temperature, °C	Leakage Conductance, 10^{-12} mho	Olivine Conductance,* 10^{-12} mho
24	1.0×10^0	1.8×10^2
100	4.0×10^1	5.1×10^2
200	7.3×10^1	1.6×10^3
300	8.9×10^1	2.2×10^4
400	9.8×10^1	1.8×10^5
500	1.0×10^2	1.9×10^6
600	2.2×10^2	5.2×10^6
700	3.9×10^2	7.7×10^6
800	4.4×10^2	1.8×10^7
900	1.7×10^3	6.1×10^7
1000	4.0×10^3	1.8×10^6
1100	1.0×10^4	3.2×10^6
1200	3.2×10^4	1.2×10^7

*Measurements above 900°C made on Fa 9.4; measurements below 900°C made on Fa 8.2.

ties. Table 4 compiles the results of wet chemical analyses of the three olivines, as well as spectrographic determination of impurities in all four natural olivines studied here. Electron-microprobe and spectrographic analyses indicated no significant difference in impurity levels of all four samples, although there was a slight calcium enrichment in the Fa 26.4. The amount of Fa 26.4 was insufficient for wet chemical analysis; thus its composition as determined by the electron microprobe is given in Table 4.

Table 4 indicates that Fa 9.4 has little or no Fe^{3+} when compared with Fa 8.2 and Fa 7.7. During chemical analysis J. Ito (personal communication, 1971) noted that the Fa 9.4 olivine was much more stable with respect to oxidation than the Fa 8.2 olivine, because the Fa 8.2 turned reddish brown rapidly and was 80% oxidized when heated to 1150°C in air for 3 hours, whereas the Fa 9.4 changed color slowly and was less than 20% oxidized after heating at 1150°C in air for 3 hours.

This analysis, coupled with the observation that oxidation of the olivine during the experiment caused increased σ owing to an increase in the intercept with no change in slope, indicates that the σ mechanism associated with the 0.7-ev slope is due to Fe^{3+} ions in the olivine structure. The σ can be the result of either the 'hopping mechanism' proposed by *Bradley et al.* [1964] or ionic motion enhanced by local charge imbalance introduced by the presence of the Fe^{3+} ion in the olivine structure.

For all samples studied here only one mechanism of σ was observed between 800°C and the temperature at which leakage conductance affected the measurements. In this respect the data agree with the observations of *Mizutani and Kanamori* [1967] for olivine from Miyake-jima (Fa 18) and *Shankland* [1969] for synthetic forsterite and disagree with the observations of *Noritomi* [1961] for olivine from Bonin Island and Sado (Fa 20) and *Hughes* [1953] for the Red Sea peridot. This disagreement can be explained as a result of differences in impurity levels of olivines from different localities and, in the case of Hughes, whose measurements were made in air, as a result of oxidation.

The variation of σ with crystal direction in the Fa 8.2 is included in Figure 2. These data are the result of linear-regression analyses of at
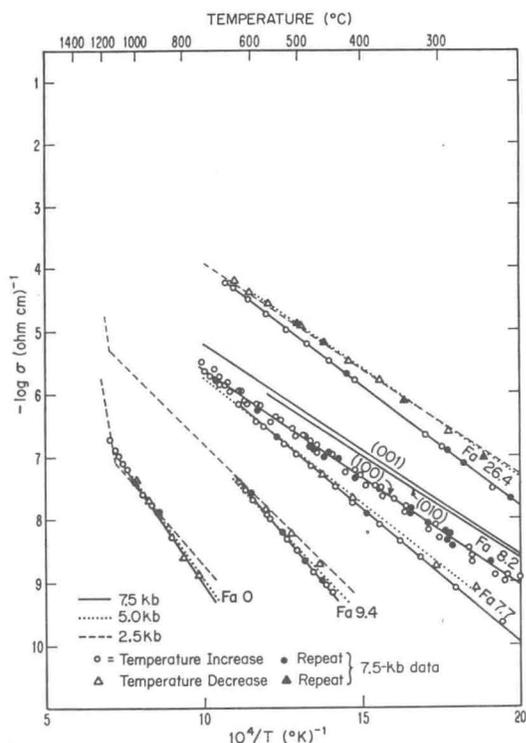
Fig. 2. Electrical conductivity of olivine as a function of temperature, pressure, composition, and crystal direction. Solid lines are for 7.5-kb data. Data points are as follows: open circles, temperature-increase measurements; shaded circles, a cycling down of 100°–200°C to check reproducibility; open triangles, measurements taken after the maximum temperature has been attained; shaded triangles, a cycling up of 100°–200°C to check reproducibility. As can be seen, most of the pressure effect can be attributed to some change in the system after the highest temperature was achieved. The small pressure effect for Fa 8.2 could not be plotted on this scale. The variation of conductivity with direction is plotted for this composition as the result of least-squares fits to at least two runs on two different sections of the same crystal in each direction. The data points for the three runs in the (100) direction are plotted. The scatter is large because of thickness and size-measurement errors among the three samples.

least two runs for each crystal direction at 7.5 kb. Although the data for individual and combined runs tend to plot in the order shown in Figure 2, the difference in σ as a function of crystallographic orientation is within the experimental accuracy, as is indicated by Table 3.

The data for the temperature region between

TABLE 3. Results of Linear-Regression Analysis of Experimental Data

osition	Crystal Direction	Pressure, kb	Temperature Range, $10^4/T$ (°K)$^{-1}$	log σ_x	A/k	Sta
7.7						
		7.50	18 to 11	-1.428	0.4272	
		5.00	19 to 10	-1.675	0.4056	
8.2						
	(100)	7.50	20 to 11	-1.764	0.3701	
	(100)	7.50	20 to 11	-2.080	0.3565	
	(100)	5.00	22 to 11	-2.036	0.3566	
	(100)	2.50	22 to 11	-2.022	0.3575	
	(100)	7.50	20 to 10	-2.135	0.3441	
	(100)	7.50	20 to 11	-2.126	0.3478	
	(010)	7.50	20 to 11	-1.571	0.3644	
	(010)	7.50	22 to 9	-1.945	0.3389	
	(010)	7.50	22 to 11	-1.931	0.3377	
	(010)	5.0	24 to 11	-1.982	0.3323	
	(010)	2.5	24 to 12	-1.711	0.3523	
	(010)	0	19 to 11	-1.910	0.3450	
	(010)	7.50	20 to 12	-1.917	0.3399	
	(001)	7.50	22 to 10	-1.735	0.3500	
	(001)	5.00	23 to 11	-1.700	0.3477	
	(001)	2.50	24 to 12.5	-1.536	0.3558	
	(001)	7.50	21 to 10	-1.646	0.3505	
	(001)	7.50	21 to 10	-1.697	0.3507	

TABLE 3.   Continued

Sample	Composition	Crystal Direction	Pressure, kb	Temperature Range, $10^4/T$ $(°K)^{-1}$	$\log \sigma_x$	A/k	Stand. Deviation	A_x, ev
St. John's Island	Fa 9.4							
35*		(010)	7.50	15 to 11	−0.6245	0.6097	0.01383	1.2097
35*		(010)	5.00	15 to 11	−1.471	0.5405	0.007261	1.0724
35*		(010)	2.50	15 to 7.3	−1.859	0.4986	0.02002	0.9893
35*		(010)	2.50	7.05 to 6.9	+20.056	3.587	2 points only	7.117
Crater Elegante	Fa 26.4							
36*			7.50	20 to 11	−0.1012	0.3855	0.009410	0.7649
36*			5.0	21 to 12	−0.3204	0.3518	0.008379	0.6980
36*			2.5	21 to 10	−0.5887	0.3349	0.01016	0.6645
Synthetic	Fa 0							
38*			7.5	9.5 to 7.2	−0.7139	0.8573	0.01300	1.701
38*			5.0	10.1 to 7.3	−1.810	0.7165	0.01213	1.422
38*			2.5	10.0 to 7.5	−2.932	0.5796	0.03838	1.150
38*§			2.5	7.15 to 6.8	+21.972	4.0284	0.23937	7.993

*Data used in Figure 6.
†Experiment repeated 2 weeks later to check reproducibility.
§Three data points used in this calculation.

TABLE 4. Results of Spectrographic, Electron-Microprobe,
and Wet Chemical Analyses of Olivine Samples
(Composition of synthetic forsterite given in Table 1.)

Oxide	Wet Chemical Analyses, wt %			Crater Elegante Microprobe Analysis,¶ wt %
	San Carlos*	Red Sea†	Mt. Leura§	
SiO_2	40.7	40.5	41.0	37.8
Al_2O_3	0.2	0.3	0.1	<0.2
Cr_2O_3	0.05	0.00x	0.02	
Fe_2O_3	0.41	||	0.34	} 24.2
FeO	7.94	9.16	7.5	
MnO	0.12	0.14	0.11	<0.2
MgO	50.1	49.3	50.7	37.7
CoO	0.02	0.01	0.01	
NiO	0.38	0.38	0.34	<0.2
CuO	0.02	0.00x	0.01	
CaO	0.07	0.01	0.04	<0.1
ZnO	0.01	0.005	0.01	
Na_2O	0.01	0.02	0.01	
K_2O	0.00	0.01	0.00	
Total	100.03	99.83	100.19	

*8.2 mole % fayalite; spectrographic trace elements Ti, Ba, Be, Sc.
†9.4 mole % fayalite; spectrographic trace elements Ti, Ba, Ag, Sc.
§7.7 mole % fayalite; spectrographic trace elements Ti, Ba, Ag, Sc.
¶26.4 mole % fayalite; spectrographic trace elements Ti, Ba, Ag, Sc.
\|\|Present but small (≤0.2%).

500° and 1100°C in the Fa 9.4 and between 700° and 1100°C in the Fa 0 indicate that only one σ mechanism is operating in these olivines in these temperature regions. It is possible that some other σ mechanism is effective at lower temperatures, but the larger leakage conductance of the sample holder masks these regions. Above about 1150°C the two olivines exhibit a large reversible increase in σ. Because of the deterioration of the chromel-alumel thermocouple, the data were collected over a small region of reciprocal temperature space and are of poor precision. However, despite large differences in initial conductivity, both samples indicate an A_x of 7–8 ev and a σ_x of 10^{21}–10^{22}. Although the poor precision does not allow more than a qualitative assessment of the nature of the difference in A_x, it would appear that the synthetic Fa 0 requires the larger A_x (8 ev) vis a vis the Fa 9.4 (7.1 ev).

Table 3 summarizes the coefficients and stand-ard deviations of the linear-regression analysis of the data for various compositions, pressures, crystal directions, and temperature ranges. For the linear-regression analysis log σ was treated as the dependent variable, and $10^4/T$ $(°K)^{-1}$ was treated as the independent variable. Log σ_x is the log pre-exponential term of (1) and is negative for all samples studied, except samples 38 and 35 from the high-temperature region, where log σ_x is 22 and 21, respectively. The term A_x/k from (1) is the slope of this 'best-fit' line, and from this term the activation energy E may be calculated. However, A_x is listed in Table 3 because its use involves no interpretation of conduction mode, as would a listing of activation energies.

Figure 3 compares the data of Figure 2 with available literature data for single crystals of olivine. With the notable exceptions of the Red Sea peridot, Sado olivine, and synthetic forsterite, there is a wide band of agreement, within

an order of magnitude, on the σ of olivine in the temperature region below 1000°C. This band is delimited by the Fa 7.7 olivine for low conductivity and the Fa 26.4 olivine for high conductivity. Besides the higher temperature measurements of the Bonin Island olivine, which have slopes similar to the Red Sea peridot, the slopes in this temperature region are similar ($A_s \cong 0.7$ ev). This similarity indicates a common mechanism of conductivity that is probably due to ferric-iron content. The steeper slopes represented by the low- temperature portions of the synthetic forsterite, Red Sea peridot, and intermediate-temperature portion of the Bonin and Sado olivines may be the result of extrinsic ionic conductivities [*Shankland*, 1969]. The mechanism of conductivity for the highest-temperature portion may be due to ionic or intrinsic electronic conductivity.

Figures 4 and 5 compare the variation of A_x and σ_x with pressure for all samples studied with literature values. Only the (001) direction for the Fa 8.2 A_x has been plotted, because all three directions are almost the same in both sign and magnitude of the variation. The pressure derivatives of σ_x for the Fa 9.4 and the Fa 0 show a significantly larger pressure effect than the other samples. Except for the Fa 8.2, all single crystals studied have derivatives that are opposite those reported for powders. One could attribute this marked variation between single crystals and powders to compaction and grain-boundary effects in the powders. However, the Fa 8.2 has derivatives in the same sense as the powders, unlike the four other compositions studied.

It is obvious from an inspection of Figure 2 that something other than pressure affected the conductivity pressure derivatives. In this figure the triangles represent low-temperature conductivity measurements made after a crystal had been at the highest temperature. In every sample but the Fa 8.2 the low-temperature data points fall at conductivities higher than those noted on the measurements made before the highest temperature was achieved. This change is in the same direction as the 'pressure effect' and could be the result of the deterioration of the thermocouple, the annealing of dislocations, the diffusion of oxygen into the crystals, or some artifact of the coating procedure, because, as noted above, the Fa 8.2 olivine was platinum-plated
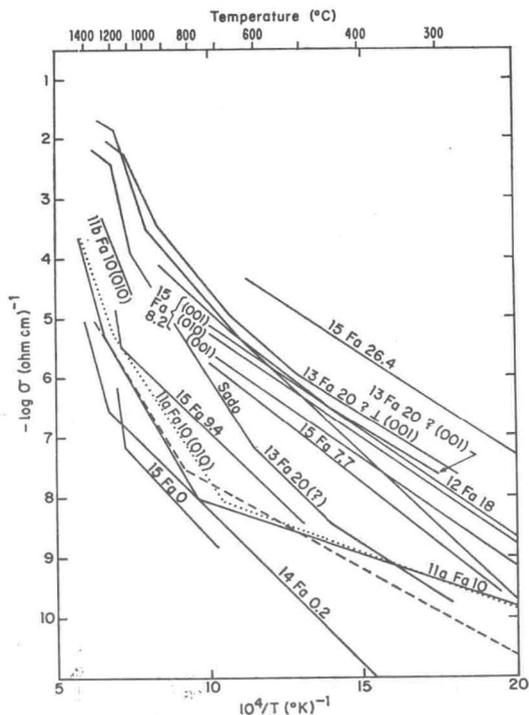
Fig. 3. Conductivity of olivine single crystals as determined by this and other studies. Composition is indicated above the line. Question mark means that the composition of olivine was not reported by the author. Numbers in parentheses give the direction in which σ measurement was made. First number above the line refers to one of the following investigators: 11*a*, *Hughes* [1953]; 11*b*, *Hughes* [1955]; 12, Mizutani and Kanamori [1967]; 13, *Noritomi* [1961]; 14, *Shankland* [1969].

in air at 600°C, whereas the other samples were plated in a vacuum at 800°C. It seems likely that a combination of the last two possibilities is the most probable cause of the variation. It is proposed that the Fa 8.2 came to equilibrium with an oxygen atmosphere during plating (however, no color change was noted in the thin uncoated plates of the sample that were present during the plating process), whereas all other samples were subjected to an oxygen-rich atmosphere only during actual measurement of conductivity.

The results of the experiments reported above can be summarized as follows:

1.   Although an increase in iron content generally increases the σ of olivine, olivines with small differences in iron content may differ by
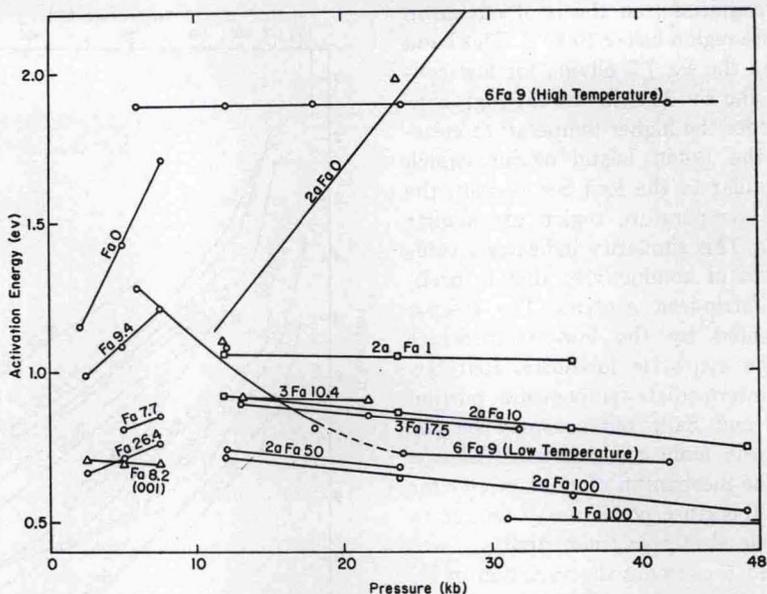
Fig. 4. Activation energy as a function of pressure, as reported for olivine powders and as determined in this study for olivine single crystals. Composition is indicated above the line. A line intersecting a boundary indicates that the data are off-scale. Numbers above the line refer to the following investigators: 1, *Akimoto and Fujisawa* [1965]; 2a, *Bradley et al.* [1964]; 3, *Hamilton* [1965]; 6, *Schult and Schober* [1969].
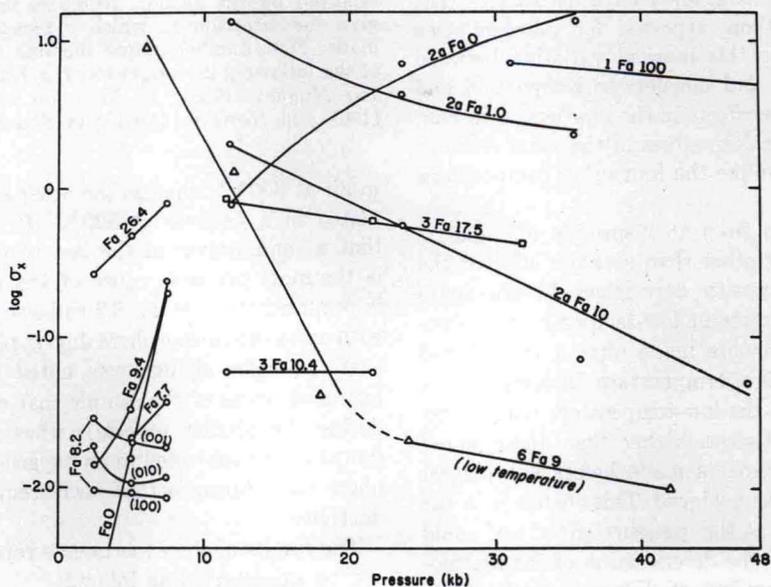
Fig. 5. Log σ_x as a function of pressure, as reported for olivine powders and as determined in this study for olivine single crystals. Composition is indicated above the line. A line intersecting a boundary indicates that the data are off-scale. Numbers above the line refer to the investigators listed in Figure 4.

orders of magnitude in σ. Further, the fayalite-poor olivine may be the better conductor.

2. In olivines with similar fayalite and impurity contents the amount of Fe^{3+} present determines the σ up to at least 800°C.

3. This study cannot claim to have determined an unambiguous pressure derivative because of experimental difficulties.

4. There is a large and reversible change in σ mechanism in olivine at about 1150°C. The activation energy and pre-exponential term for this mechanism, as determined by various laboratories, vary from 3 to 8 ev and 10^6 to 10^{22}, respectively.

5. For all natural olivines studied here, except the Fa 9.4, no change in mechanism indicated by a reversible change of slope was observed between 200° and 800°C. The Fa 9.4 and the Fa 0 have no change in mechanism between 500° and 1100°C.

GEOPHYSICAL APPLICATIONS

The present data on the σ of olivine single crystals can be used to estimate the temperature at depth in the mantle if (1) is solved for T (degrees Kelvin):

$$T = \frac{A_x \log e}{k(\log \sigma_x - \log \sigma_m)} \quad (3)$$

where $\log \sigma_m$ is the σ of the mantle. Both the magnetotelluric σ profile of *Eckhardt et al.* [1963] and the geomagnetic profile of *McDonald* [1957] were used in these calculations.

If the pressure derivatives of A_x and $\log \sigma_x$ are substituted in (3), the temperature at depth T_p is

$$T_p = \frac{\left[A_x + \left(\frac{dA_x}{dP}\right)_T P \right] \log e}{k \left[\log \sigma_x + \left(\frac{d \log \sigma_x}{dP}\right)_T P - \log \sigma_m \right]} \quad (4)$$

Figure 6 shows the temperature calculated from the present data for 40, 100, 200, and 400 km from (3) and (4). The calculations for Fa 10 olivines with no pressure effect yield temperatures that are significantly higher than those proposed for the mantle beneath both the oceans and the shields [*Ringwood*, 1966; *Clark and Ringwood*, 1964] at any depth. In fact, these temperatures are sufficient to activate the high-temperature conductivity mechanism that
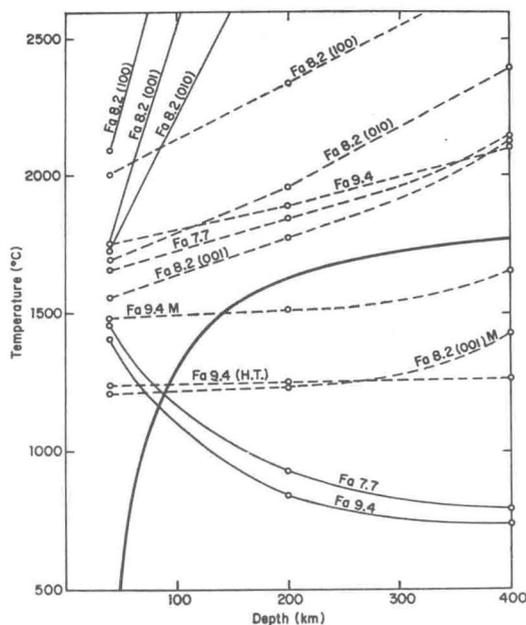
Fig. 6. Temperature distribution in the mantle. Heavy solid line is the oceanic geotherm of *Ringwood* [1966], extrapolated beyond the 250-km depth on the basis of data from *Clark and Ringwood* [1964]. The thin solid lines connect temperature points calculated by using the pressure derivatives obtained in this study and the Cantwell-McDonald profile of σ depth. Broken lines connect temperature points calculated without using pressure derivatives. *M* refers to temperature points based on the McDonald profile of conductivity depth, and H. T. refers to the temperature calculations based on the high-temperature mechanism observed in Fa 9.4. Composition of olivine is indicated above the line, and the numbers in parentheses indicate the crystal direction of the σ measurement.

was observed for the Fa 9.4 and the Fa 0. Thus Figure 6 also includes calculations based on these high-temperature σ mechanisms.

The pressure effect observed for the low-temperature σ mechanism causes the calculated temperature to decrease with depth, except in the case of the Fa 8.2, and indicates a temperature at 400 km that is somewhat lower than has been proposed for the mantle beneath either the oceanic or the shield areas. The pressure effect observed for the Fa 8.2 yields a temperature distribution that is much larger than expected for the mantle.

This study shows that the σ is quite variable among olivines with compositions close to the

assumed composition of olivine in the mantle (Fa 10). Thus, even if one neglects the uncertainties introduced by grain boundaries, the calculation of temperature distributions at depth based on magnetic and laboratory σ data [see *England et al.*, 1968; *Tozer*, 1959] is subject to large uncertainties. The uncertainty is further increased if the possible effects of pressure and the uncertainties in the σ distribution in the mantle [*Parker*, 1971] are taken into account.

REFERENCES

Akimoto, S., and H. Fujisawa, Demonstration of the electrical-conductivity jump produced by the olivine-spinel transition, *J. Geophys. Res.*, 70, 443–449, 1965.

Banks, R. J., Geomagnetic variations and the electrical conductivity of the upper mantle, *Geophys. J. Roy. Astron. Soc.*, 17, 457–487, 1969.

Birch, F., Density and composition of the upper mantle: First approximation as an olivine layer, in *The Earth's Crust and Upper Mantle, Geophys. Monogr. Ser.*, vol. 13, edited by P. J. Hart, pp. 18–36, AGU, Washington, D.C., 1969.

Bradley, R. S., A. K. Jamil, and D. C. Munro, The electrical conductivity of fayalite and spinel, *Nature, 193*, 965–966, 1962.

Bradley, R. S., A. K. Jamil, and D. C. Munro, The electrical conductivity of olivine at high temperatures and pressures, *Geochim. Cosmochim. Acta, 28*, 1669–1678, 1964.

Clark, S. P., Jr., and A. E. Ringwood, Density distribution and constitution of the mantle, *Rev. Geophys. Space Phys., 2*, 35–88, 1964.

Dekker, A. J., *Solid State Physics*, pp. 160–182, 305–346, Prentice-Hall, Englewood Cliffs, N.J., 1958.

Eckhardt, D., K. Larner, and T. Madden, Long-period magnetic fluctuations and mantle conductivity estimates, *J. Geophys. Res., 68*, 6279–6286, 1963.

England, A. W., G. Simmons, and D. Strangway, Electrical conductivity of the moon, *J. Geophys. Res., 73*, 3219–3226, 1968.

Fujisawa, H., Temperature and discontinuities in the transition layer within the earth's mantle: Geophysical application of the olivine-spinel transition in the Mg_2SiO_4–Fe_2SiO_4 system, *J. Geophys. Res., 73*, 3281–3294, 1968.

Getting, I. C., and G. C. Kennedy, The effect of pressure on the emf of chromel-alumel and platinum-platinum 10% rhodium thermocouples, in *Proceedings of a Symposium on the Accurate Characterization of the High Pressure Environment*, pp. 77–80, National Bureau of Standards, Washington, D.C., 1971.

Hamilton, R. M., Temperature variation at constant pressure of the electrical conductivity of periclase and olivine, *J. Geophys. Res., 70*, 5679–5692, 1965.

Harris, P. G., A. Reay, and I. G. White, Chemical composition of the upper mantle, *J. Geophys. Res., 72*, 6359–6369, 1967.

Hughes, H., The electrical conductivity of the earth's interior, Ph.D. thesis, Univ. of Cambridge, Cambridge, England, 1953.

Hughes, H., The pressure effect on the electrical conductivity of peridot, *J. Geophys. Res., 60*, 187–191, 1955.

Hutson, A. R., Semiconducting properties of some oxides and sulfides, in *Semiconductors*, edited by N. B. Hannay, pp. 541–599, Reinhold, New York, 1959.

Jander, W., and W. Stamm, Der innere aufbau fester anorganischer verbindungen bei hoheren temperature, *Z. Anorg. Allg. Chem., 207*, 289–307, 1932.

Kittel, C., *Introduction to Solid State Physics*, 3rd ed., pp. 301–330, John Wiley, New York, 1966.

Kumazawa, M., and O. L. Anderson, Elastic moduli, pressure derivatives and temperature derivatives of single-crystal olivine and single-crystal forsterite, *J. Geophys. Res., 74*, 5961–5972, 1969.

McDonald, K. L., Penetration of the geomagnetic secular field through a mantle with variable conductivity, *J. Geophys. Res., 62*, 117–141, 1957.

Mizutani, H., and H. Kanamori, Electrical conductivities of rock forming minerals at high temperatures, *J. Phys. Earth, 15*, 25–31, 1967.

Noritomi, K., The electrical conductivity of rocks and the determination of electrical conductivity of the earth's interior, *J. Mining Coll. Akita Univ., Ser. A, 1*, 27–59, 1961.

Parker, R. L., The inverse problem of electrical conductivity in the mantle, *Geophys. J. Roy. Astron. Soc., 22,* 121–138, 1971.

Pluschkell, W., and H. J. Engell, Ionen-und elektronenleitung im magnesium-orthosilikat, *Ber. Deut. Keram. Ges., 45,* 388–394, 1968.

Price, A. T., Magnetic variations and telluric currents, in *The Earth's Mantle,* edited by T. F. Gaskell, pp. 125–170, Academic, New York, 1967.

Ringwood, A. E., Mineralogy of the mantle, in *Advances in Earth Science,* edited by P. M. Hurley, pp. 357–399, MIT Press, Cambridge, Mass., 1966.

Ringwood, A. E., Composition and evolution of the upper mantle, in *The Earth's Crust and Upper Mantle, Geophys. Monogr. Ser.,* vol. 13, edited by P. J. Hart, pp. 1–17, AGU, Washington, D. C., 1969.

Rodgers, D., A. Ferretti, and W. Kunnman, Single crystal growth and electrical transport properties of intermediates in the spinel system $Co_{1+\delta}V_{2-\delta}O_4$, *J. Phys. Chem. Solids, 27,* 1445–1451, 1966.

Schock, R. N., Diffusion in a pressure gradient, Ph.D. thesis, Rensselaer Polytech. Inst., Troy, N. Y., 1966.

Schult, A., and M. Schober, Measurement of electrical conductivity of natural olivine at temperatures up to 950°C and pressures up to 42 kilobars, *Z. Geophys., 35,* 105–112, 1969.

Shankland, T. J., Transport properties of olivine, in *The Application of Modern Physics to the Earth and Planetary Interiors,* edited by S. K. Runcorn, pp. 175–190, Interscience, New York, 1969.

Tozer, D. C., The electrical properties of the earth's interior, *Phys. Chem. Earth, 3,* 414–436, 1959.

Volarovich, M. P., E. A. Parkhomenko, and A. T. Bondarenko, Investigation of electrical resistance of basic, ultrabasic, and alkaline rocks and minerals at high pressures and temperatures, *Tr. Inst. Fiz. Zemli Akad. Nauk SSSR,* no. 37, 168–179, 1966. (*NASA Tech. Transl. TT F-13, 212,* 1–20, 1970.)

Wyllie, P. J., Ultramafic rocks and the upper mantle, *Spec. Pap. 3,* pp. 3–32, Mineral. Soc. of Amer., Washington, D. C., 1970.